Meteorological modes of variability for fine particulate matter (PM[subscript 2.5]) air quality in the United States: implications for PM[subscript 2.5] sensitivity to climate change

Atmos. Chem. Phys., 12, 3131–3145, 2012
www.atmos-chem-phys.net/12/3131/2012/
doi:10.5194/acp-12-3131-2012

Atmospheric Chemistry and Physics

Meteorological modes of variability for fine particulate matter ($PM_{2.5}$) air quality in the United States: implications for $PM_{2.5}$ sensitivity to climate change

A. P. K. Tai[1], L. J. Mickley[1], D. J. Jacob[1], E. M. Leibensperger[2], L. Zhang[1], J. A. Fisher[1], and H. O. T. Pye[3]

[1]School of Engineering and Applied Sciences, Harvard University, Cambridge, Massachusetts, USA
[2]Department of Earth, Atmospheric and Planetary Sciences, Massachusetts Institute of Technology, Cambridge, Massachusetts, USA
[3]National Exposure Research Laboratory, US Environmental Protection Agency, Research Triangle Park, North Carolina, USA

Correspondence to: A. P. K. Tai (tai@seas.harvard.edu)

Received: 15 September 2011 – Published in Atmos. Chem. Phys. Discuss.: 22 November 2011
Revised: 13 March 2012 – Accepted: 21 March 2012 – Published: 30 March 2012

Abstract. We applied a multiple linear regression model to understand the relationships of $PM_{2.5}$ with meteorological variables in the contiguous US and from there to infer the sensitivity of $PM_{2.5}$ to climate change. We used 2004–2008 $PM_{2.5}$ observations from ∼1000 sites (∼200 sites for $PM_{2.5}$ components) and compared to results from the GEOS-Chem chemical transport model (CTM). All data were deseasonalized to focus on synoptic-scale correlations. We find strong positive correlations of $PM_{2.5}$ components with temperature in most of the US, except for nitrate in the Southeast where the correlation is negative. Relative humidity (RH) is generally positively correlated with sulfate and nitrate but negatively correlated with organic carbon. GEOS-Chem results indicate that most of the correlations of $PM_{2.5}$ with temperature and RH do not arise from direct dependence but from covariation with synoptic transport. We applied principal component analysis and regression to identify the dominant meteorological modes controlling $PM_{2.5}$ variability, and show that 20–40 % of the observed $PM_{2.5}$ day-to-day variability can be explained by a single dominant meteorological mode: cold frontal passages in the eastern US and maritime inflow in the West. These and other synoptic transport modes drive most of the overall correlations of $PM_{2.5}$ with temperature and RH except in the Southeast. We show that interannual variability of $PM_{2.5}$ in the US Midwest is strongly correlated with cyclone frequency as diagnosed from a spectral-autoregressive analysis of the dominant meteorological mode. An ensemble of five realizations of 1996–2050 climate change with the GISS general circulation model (GCM) using the same climate forcings shows inconsistent trends in cyclone frequency over the Midwest (including in sign), with a likely decrease in cyclone frequency implying an increase in $PM_{2.5}$. Our results demonstrate the need for multiple GCM realizations (because of climate chaos) when diagnosing the effect of climate change on $PM_{2.5}$, and suggest that analysis of meteorological modes of variability provides a computationally more affordable approach for this purpose than coupled GCM-CTM studies.

1 Introduction

Air pollution is highly dependent on weather, and it follows that climate change could significantly impact air quality. The pollutants of most public health concern are ozone and fine particulate matter with diameter less than 2.5 µm ($PM_{2.5}$). Studies using chemical transport models (CTMs) driven by general circulation models (GCMs) consistently project a worsening of ozone air quality in a warming climate (Weaver et al., 2009). This finding is buttressed by observed correlations of ozone with temperature that are well reproduced by models (Jacob et al., 1993; Sillman and Samson, 1995; Rasmussen et al., 2012). By contrast, GCM-CTM studies of the effect of climate change on $PM_{2.5}$ show no consistency even in the sign of effect (Jacob and Winner, 2009). In previous work (Tai et al., 2010), we examined

the observed correlations of $PM_{2.5}$ and its components in the US with meteorological variables as a means to understand $PM_{2.5}$ response to climate change. Here we develop this approach further to define meteorological modes of variability for $PM_{2.5}$ and interpret the observed correlations and modes using the GEOS-Chem CTM. We apply the Goddard Institute for Space Studies (GISS) GCM to illustrate how the modes enable effective diagnosis of the effect of climate change on $PM_{2.5}$.

The uncertainty in assessing climatic effects on $PM_{2.5}$ reflects the complex dependence of different $PM_{2.5}$ components on meteorological variables. Higher temperatures can lead to higher sulfate concentrations due to faster SO_2 oxidation, but to lower nitrate and organic components due to volatility (Sheehan and Bowman, 2001; Aw and Kleeman, 2003; Dawson et al., 2007; Kleeman, 2008). Biogenic emissions of $PM_{2.5}$ precursors including agricultural ammonia, soil NO_x, and volatile organic compounds (VOCs) increase with temperature and further complicate the $PM_{2.5}$-temperature relationship (Pinder et al., 2004; Bertram et al., 2005; Guenther et al., 2006). Higher relative humidity (RH) promotes aqueous-phase sulfate production and ammonium nitrate formation (Koch et al., 2003; Liao et al., 2006; Dawson et al., 2007), but inhibits fires, which are important contributors to organic aerosols in many regions (Park et al., 2007; Spracklen et al., 2009). Changes in precipitation and in planetary boundary layer (PBL) depth have a consistent effect on $PM_{2.5}$ components but their projections in GCMs are highly uncertain (Jacob and Winner, 2009).

Synoptic-scale transport should be an important factor driving the effect of climate change on $PM_{2.5}$. Previous studies have used principal component analysis (PCA) to identify important meteorological modes of variability for $PM_{2.5}$ air quality (Cheng et al., 2007; Thishan Dharshana et al., 2010). Thishan Dharshana et al. (2010) found that as much as 30 % of $PM_{2.5}$ daily variability in the US Midwest is associated with passages of synoptic weather systems. Cold fronts associated with mid-latitude cyclone passages provide the dominant ventilation pathway for the eastern US (Cooper et al., 2001; Li et al., 2005). A general reduction in the frequency of these cyclones is expected as a result of greenhouse warming (Lambert and Fyfe, 2006; Christensen et al., 2007; Pinto et al., 2007), potentially leading to more frequent and prolonged stagnation episodes (Mickley et al., 2004; Murazaki and Hess, 2006). Leibensperger et al. (2008) found a strong anticorrelation between summer cyclone frequency and ozone pollution in the eastern US for 1980–2006, and further showed evidence of a long-term decline in cyclone frequency over that period that significantly hindered attainment of ozone air quality standards. Tai et al. (2010) projected a $PM_{2.5}$ enhancement of up to $1\,\mu g\,m^{-3}$ in the Midwest from 2000–2050 climate change due to more frequent stagnation.

In this study, we first apply the GEOS-Chem global CTM to interpret the observed correlations between $PM_{2.5}$ components and meteorological variables in the contiguous US. As we will see, interpretation is complicated by the covariation of meteorological variables with synoptic transport. To address this issue, we use PCA and regression to determine the dominant meteorological modes of observed daily $PM_{2.5}$ variability in different US regions, and show how spectral analysis of these modes enables a robust estimate of the effect of climate change on $PM_{2.5}$ air quality.

2 Data and models

2.1 $PM_{2.5}$ observations

Daily mean surface concentrations of total $PM_{2.5}$ and speciated components including sulfate, nitrate, and organic carbon (OC) for 2004–2008 were obtained from the ensemble of sites of the EPA Air Quality System (EPA-AQS) (http://www.epa.gov/ttn/airs/airsaqs/), shown in Fig. 1. Total $PM_{2.5}$ data are from the Federal Reference Method (FRM) network of about 1000 sites in the contiguous US. Speciation data are from the State and Local Air Monitoring Stations (SLAMS) and Speciation Trends Network (STN) of about 200 sites. These sites measure every one, three or six days. Tai et al. (2010) show maps of the annual mean data for total $PM_{2.5}$ (1998–2008) and individual components (2000–2008). We do not discuss ammonium and elemental carbon (EC) here because ammonium is mainly the counter-ion for sulfate and nitrate, and the correlation patterns of EC with meteorological variables generally follow those of OC (Tai et al., 2010).

2.2 GEOS-Chem simulations

We used the GEOS-Chem global CTM to conduct full-year simulations of coupled gas-phase and aerosol chemistry. GEOS-Chem (http://geos-chem.org) uses assimilated meteorological data from the NASA Global Earth Observing System (GEOS-5) with 6-h temporal resolution (3-h for surface variables and PBL depth), 0.5° latitude by 0.667° longitude ($0.5^\circ \times 0.667^\circ$) horizontal resolution, and 47 hybrid pressure-sigma vertical levels. We conducted GEOS-Chem simulations at three different horizontal resolutions: native $0.5^\circ \times 0.667^\circ$, $2^\circ \times 2.5^\circ$, and $4^\circ \times 5^\circ$. The coarser resolutions have been used previously with meteorological fields from the GISS GCM to investigate effects of climate change on air quality (Wu et al., 2008; Pye et al., 2009; Leibensperger et al., 2011a). For the native resolution simulation we used a nested continental version of GEOS-Chem over North America (140–40° W, 10–70° N) with $2^\circ \times 2.5^\circ$ resolution for the rest of the world (Chen et al., 2009; Zhang et al., 2011). The native simulation was conducted for one year (2006) and the $2^\circ \times 2.5^\circ$ and $4^\circ \times 5^\circ$ simulations for three years (2005–2007) using GEOS-Chem version 8-3-2. We included a non-local PBL mixing scheme formulated

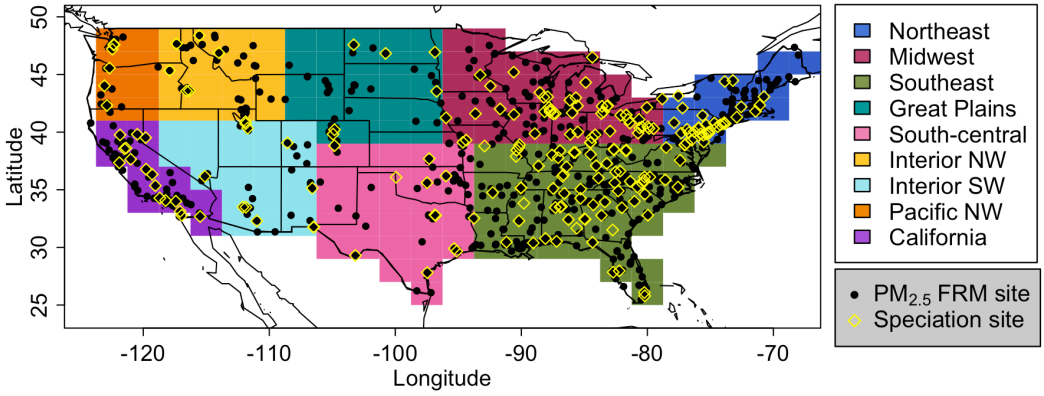

Fig. 1. US regions used to study the correlations of $PM_{2.5}$ with meteorological modes of variability. Also shown are the EPA Air Quality System (AQS) $PM_{2.5}$ monitoring sites in 2006, including total $PM_{2.5}$ monitors using the Federal Reference Method (FRM) and chemical speciation monitors from the SLAMS + STN networks.

by Holtslag and Boville (1993) and implemented in GEOS-Chem by Lin and McElroy (2010). GEOS-Chem includes a fully coupled treatment of tropospheric ozone-NO_x-VOC-aerosol chemistry (Park et al., 2004; Liao et al., 2007). Gas-aerosol phase partitioning of the sulfate-nitrate-ammonium-water system is calculated using the ISORROPIA II thermodynamic equilibrium model (Fountoukis and Nenes, 2007). In-cloud SO_2 oxidation uses liquid water content information from the GEOS-5 archive (Fisher et al., 2011). Secondary organic aerosol (SOA) formation is computed with a standard mechanism based on reversible gas-aerosol partitioning of semi-volatile VOC oxidation products (Chung and Seinfeld, 2002). SOA precursors include isoprene, terpenes, and aromatic hydrocarbons (Henze et al., 2008).

Anthropogenic emissions of sulfur, ammonia and NO_x emissions in the US are from the EPA 2005 National Emissions Inventory (http://www.epa.gov/ttn/chief/net/2005inventory.html), and primary anthropogenic OC and EC emissions are from Cooke et al. (1999). Non-US anthropogenic emissions are described by Park et al. (2006). Biomass burning emissions of OC and EC are from the Global Fire Emissions Database (GFED v2) (Giglio et al., 2006). These emissions are included in the model as monthly averages and do not contribute to day-to-day variability of $PM_{2.5}$. In contrast, soil NO_x emissions (Yienger and Levy, 1995) and biogenic emissions of isoprene, terpenes, and methylbutenol (Guenther et al., 2006) are updated locally every three hours as a function of temperature, solar radiation, and precipitation. Scavenging of $PM_{2.5}$ by precipitation follows the scheme of Liu et al. (2001). Dry deposition follows a standard resistance-in-series scheme (Wesely, 1989) as implemented by Wang et al. (1998).

Maps of annual mean $PM_{2.5}$ concentrations from our simulation are included in the Supplement. Total $PM_{2.5}$ in GEOS-Chem is taken to be the sum of sulfate, nitrate, ammonium, OC and EC. Detailed evaluations of the GEOS-Chem simulation of $PM_{2.5}$ and its components over the US have been presented in a number of publications using observations from surface sites, aircraft, and satellites (Heald et al., 2006, 2008; Park et al., 2006; van Donkelaar et al., 2006, 2008; Fu et al., 2009; Drury et al., 2010; Leibensperger et al., 2011a; Zhang et al., 2012). These evaluations mainly focused on seasonal concentrations and showed no prominent biases. Here we will focus on the ability of the model to reproduce observed correlations of $PM_{2.5}$ with meteorological variables.

2.3 Multiple linear regression

We examined the correlations of $PM_{2.5}$ and its components with meteorological variables for 2004–2008 (EPA-AQS) and 2005–2007 (GEOS-Chem) by applying a standardized multiple linear regression (MLR) model:

$$\frac{y(t)-\bar{y}}{s_y} = \sum_{k=1}^{8} \beta_k \frac{x_k(t)-\bar{x}_k}{s_k} \quad (1)$$

where y represents the deseasonalized daily $PM_{2.5}$ concentration (total $PM_{2.5}$ or individual component), x_k represents the eight deseasonalized meteorological variables from GEOS-5 listed in Table 1, $\bar{x}_k$ and $\bar{y}$ are the temporal means of x_k and y, s_k and s_y are their standard deviations (see Supplement), β_k is the dimensionless, normalized regression coefficient, and t is time. To compare observed with simulated correlations, we interpolate the EPA-AQS data onto the GEOS-Chem grid (Tai et al., 2010) and use the interpolated $PM_{2.5}$ fields for regression.

The MLR model is applied to each individual grid cell for both the observed and simulated $PM_{2.5}$ fields. All data (x_k and y) are deseasonalized and detrended by subtracting the 30-day moving averages from the original data so that

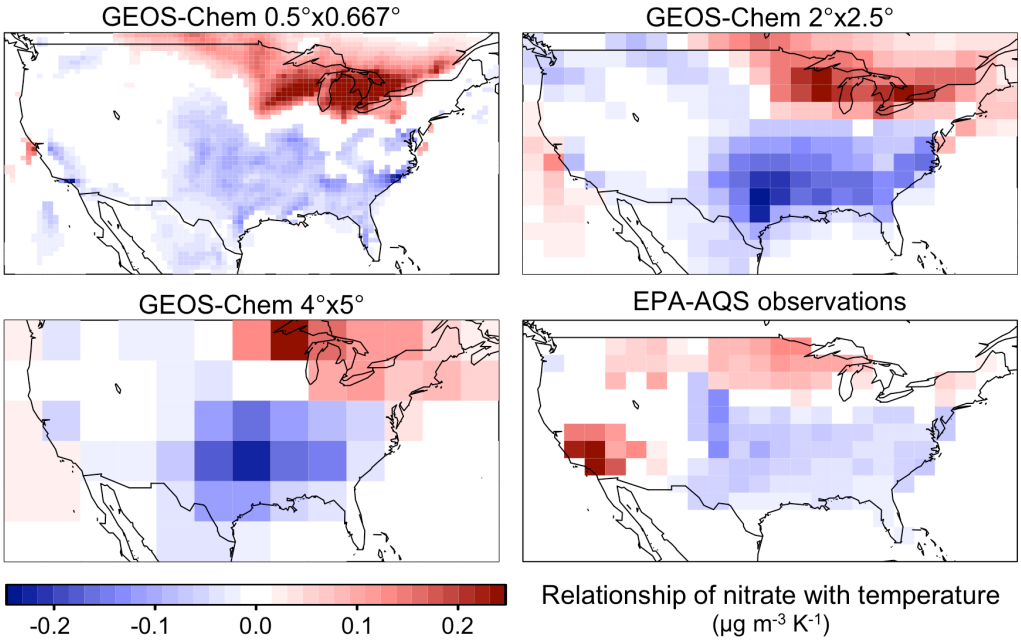

Fig. 2. Simulated (2005–2007) and observed (2004–2008) relationships of nitrate $PM_{2.5}$ with surface air temperature, as measured by the multiple linear regression coefficient β_1* in Eq. (2) with units of $\mu g\,m^{-3}\,K^{-1}$. Simulated relationships are shown for three different GEOS-Chem model resolutions: $0.5° \times 0.667°$, $2° \times 2.5°$ and $4° \times 5°$. Observations are averaged over the $2° \times 2.5°$ grid. Values are for deseasonalized and detrended variables and are only shown when significant with 95 % confidence (p-value < 0.05).

$\bar{x}_k = \bar{y} = 0$. This allows us to focus on synoptic-scale variability and avoid aliasing from common seasonal or interannual variations. The standardized regression coefficients β_k allow direct comparisons between the correlations of different $PM_{2.5}$ components with different meteorological variables (Kutner et al., 2004). The original regression coefficients β_k* in units of $\mu g\,m^{-3}\,D^{-1}$, where D is the dimension of meteorological variable x_k in Table 1, can be recovered by

$$\beta_k^* = \frac{s_y}{s_k}\beta_k \quad (2)$$

The observed coefficients of determination (R^2) for the MLR model have values ranging from 0.1 (in the west-central US where data are sparse) to 0.5 (in the Midwest and Northeast), agreeing with previous studies (Wise and Comrie, 2005; Tai et al., 2010). In addition to the standardized MLR analysis, we also conducted a stepwise MLR analysis with interaction terms as described by Tai et al. (2010). The interaction terms were generally found to be insignificant.

We conducted the MLR analysis for the model at all three resolutions ($0.5° \times 0.667°$, $2° \times 2.5°$, $4° \times 5°$) and found the patterns of correlations to be similar. Figure 2 shows as an example (to be discussed later) the simulated and observed relationships of nitrate with temperature as measured by the recovered regression coefficient β_1* in Eq. (2). In general, $2° \times 2.5°$ and $4° \times 5°$ regression results agree well with each other for all meteorological variables and all components. The native-resolution regression does not show as extensive and significant correlations. A likely explanation is that averaging over larger grid cells smoothes out local effects, yielding more robust correlation statistics. We will use $2° \times 2.5°$ resolution for model-observation comparisons in what follows.

Table 1. Meteorological variables used for $PM_{2.5}$ correlation analysis[a].

Variable	Meteorological parameter
x_1	Surface air temperature (K) [b]
x_2	Surface air relative humidity (%) [b]
x_3	Surface precipitation ($mm\,d^{-1}$)
x_4	Geopotential height at 850 hPa (km)
x_5	Sea level pressure tendency dSLP/dt ($hPa\,d^{-1}$)
x_6	Surface wind speed ($m\,s^{-1}$)[b,c]
x_7	East-west wind direction indicator cos θ (dimensionless) [d]
x_8	North-south wind direction indicator sin θ (dimensionless) [d]

[a] Assimilated meteorological data with $0.5 \times 0.667°$ horizontal resolution from the NASA Goddard Earth Observing System (GEOS-5). All data used are 24-h averages, and are deseasonalized and detrended as described in the text.
[b] At 6 m above the surface (0.994 sigma level).
[c] Calculated from the horizontal wind vectors (u, v).
[d] θ is the angle of the horizontal wind vector counterclockwise from the east. Positive values of x_7 and x_8 indicate westerly and southerly winds, respectively.

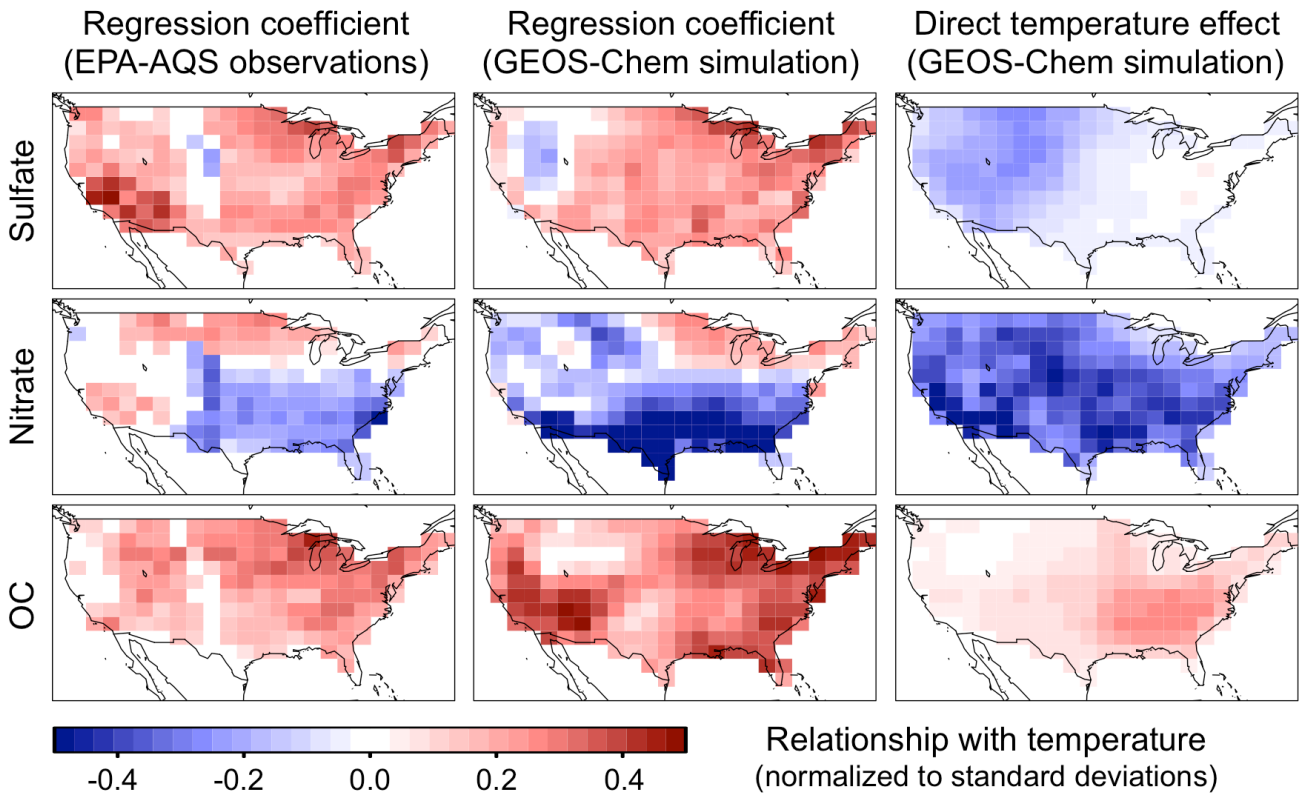

Fig. 3. Relationships of sulfate, nitrate, and organic carbon (OC) $PM_{2.5}$ concentrations with surface air temperature. The left and middle panels show the observed (2004–2008) and simulated (2005–2007) standardized regression coefficients β_1 in Eq. (1). Values are for deseasonalized and detrended variables and are only shown when significant with 95 % confidence (p-value < 0.05). The right panels show the direct effects of temperature on sulfate, nitrate and OC as determined by applying a global +1 K temperature perturbation in the GEOS-Chem simulation, and normalizing the results to the standard deviations of deseasonalized concentrations and temperatures to allow direct comparison to β_1.

3 Correlations of $PM_{2.5}$ with meteorological variables

3.1 Correlations with temperature

Figure 3 (left and middle panels) shows the observed and simulated relationships of sulfate, nitrate, and OC with temperature as measured by the standardized regression coefficient β_1 in Eq. (1). The relationships may reflect both a direct dependence of $PM_{2.5}$ on temperature and a covariation of temperature with other meteorological variables affecting $PM_{2.5}$. To separate the two effects, we conducted a direct sensitivity analysis with GEOS-Chem by increasing temperatures by 1 K throughout the troposphere while keeping all other meteorological variables constant. The resulting sensitivities are shown in the right panels of Fig. 3, normalized to the standard deviations of deseasonalized concentrations and temperature to make them directly comparable to the standardized regression coefficients β_1 in the left and middle panels.

Sulfate in the observations shows a positive relationship with temperature over most of the US. The model is generally consistent with the observations but does not capture the Southwest maximum. Results from the direct sensitivity analysis, however, show a generally negative dependence of sulfate on temperature particularly in the West. This contrasts with a previous CTM sensitivity analysis by Dawson et al. (2007) that found a positive dependence of sulfate on temperature, though much weaker than the observed relationship (Tai et al., 2010). Dawson et al. (2007) attributed their result to faster SO_2 oxidation kinetics at higher temperature, but we find in GEOS-Chem that this is more than offset by the increased volatility of H_2O_2 and SO_2, slowing down the in-cloud aqueous-phase production of sulfate. In any case, it is clear from the model that the observed positive relationship of sulfate with temperature must reflect covariation of temperature with meteorological variables rather than a direct dependence. We elaborate on this in Sect. 4.

Nitrate in the observations shows a negative relationship with temperature in the Southeast but a positive relationship

in the North and the Southwest. The model reproduces these results except for the positive relationship in the Southwest. The negative relationship in the model is too strong in the South but the higher-resolution $0.5^\circ \times 0.667^\circ$ simulation does not show such a bias (Fig. 2). The direct sensitivity of nitrate to temperature in the model is negative everywhere, with magnitude comparable to that found by Dawson et al. (2007), and reflecting the volatility of ammonium nitrate (Stelson and Seinfeld, 1982). We see from Fig. 3 that this direct dependence could account for most of the observed negative relationship of nitrate with temperature in the Southeast, but it is more than offset in the North by the positive association of temperature with southerly flow importing polluted air. The observed positive relationship of nitrate with temperature in the Southwest may reflect the temperature dependence of ammonia and fire emissions; in the model these emissions are specified as monthly means.

OC in the observations shows a positive relationship with temperature throughout the US, and the same is found in the model although the relationship is steeper. The direct sensitivity study in the model also shows a positive dependence of OC on temperature. Dawson et al. (2007) previously found a negative dependence due to OC volatility but did not consider the temperature dependence of biogenic VOC emissions, which is included in our analysis and more than offsets the volatility effect. Day and Pandis (2011) similarly found an increase in OC at higher temperatures mainly due to increased VOC emissions. We see from Fig. 3 that the direct temperature dependence may be a significant contributor the positive relationship between OC and temperature in the Southeast, where biogenic emissions are particularly high, but it has little effect elsewhere.

3.2 Correlations with relative humidity

Figure 4 shows the observed and simulated correlations of sulfate, nitrate, and OC with RH, expressed as the standardized regression coefficient β_2 in Eq. (1). The relationships are generally positive for sulfate and nitrate both in the observations and the model. The OC-RH relationship is generally negative with some model biases in the Great Plains and Midwest. Results from a model perturbation simulation similar to that for temperature are also shown in Fig. 4, indicating negligible direct dependence of sulfate and OC on RH, but a significant positive relationship for nitrate due to more favorable ammonium nitrate formation at higher RH (Stelson and Seinfeld, 1982). The direct positive sensitivity of nitrate in the southeastern coast is offset by the negative influence from the association of high RH with clean marine air, leading to the weak overall correlation there.

3.3 Correlations with precipitation and wind speed

Figure 5 shows the observed and simulated relationships of total $PM_{2.5}$ with precipitation and wind speed as measured by β_3 and β_6 in Eq. (1). Similar effects are found for all individual $PM_{2.5}$ components (Tai et al., 2010). The observations show strong negative relationships reflecting aerosol scavenging and ventilation. These are generally well captured by the model. The precipitation effect appears to be primarily driven by large-scale rather than convective precipitation in the US. Fang et al. (2011) similarly illustrated the dominance of large-scale precipitation in wet scavenging of soluble pollutants.

4 Major meteorological modes controlling $PM_{2.5}$ variability

Results from the previous section show that much of the correlation of $PM_{2.5}$ with individual meteorological variables is driven by covariance between meteorological variables, with an apparent major contribution from synoptic transport. To resolve this covariance we turn to principal component analysis (PCA) of the meteorological variables to identify the meteorological modes controlling $PM_{2.5}$ variability.

4.1 Principal component analysis and regression

We conducted a PCA for the 2004–2008 GEOS-5 data by averaging spatially over each region of Fig. 1 the eight deseasonalized meteorological variables of Table 1. The resulting time series for each region were decomposed to produce time series of eight orthogonal principal components (PCs) $(U_1, \ldots, U_8)$:

$$U_j(t) = \sum_{k=1}^{8} \alpha_{kj} \frac{X_k(t) - \bar{X}_k}{s_k} \quad (3)$$

where X_k represents the regionally averaged GEOS-5 variable, $\bar{X}_k$ and s_k the temporal mean and standard deviation of X_k,, and α_{kj} the elements of the orthogonal transformation matrix. Each PC represents a distinct meteorological regime or mode. We identified the nature of meteorological mode by examining the values of α_{kj} in Eq. (3). PCs with high $|\alpha_{kj}|$ values (e.g., greater than 0.3 and topping the other $|\alpha_{kj}|$ values) for geopotential height, pressure tendency, and wind direction are presumably associated with synoptic-scale weather systems, and can be referred to as synoptic transport modes. We then followed $U_j(t)$ day by day and visually examined the corresponding weather maps for multiple months during 2004–2008. From this we assigned a generalized meteorological feature for a given PC when the same feature could be associated with the majority of peaks and troughs of $U_j(t)$. The PCs are ranked by their variances, usually with the leading three or four PCs capturing most of the meteorological variability. For instance, in the eastern US, a single mode representing cyclone and cold frontal passages (discussed further in Sect. 4.2) typically accounts for $\sim$20 % of total meteorological variability.

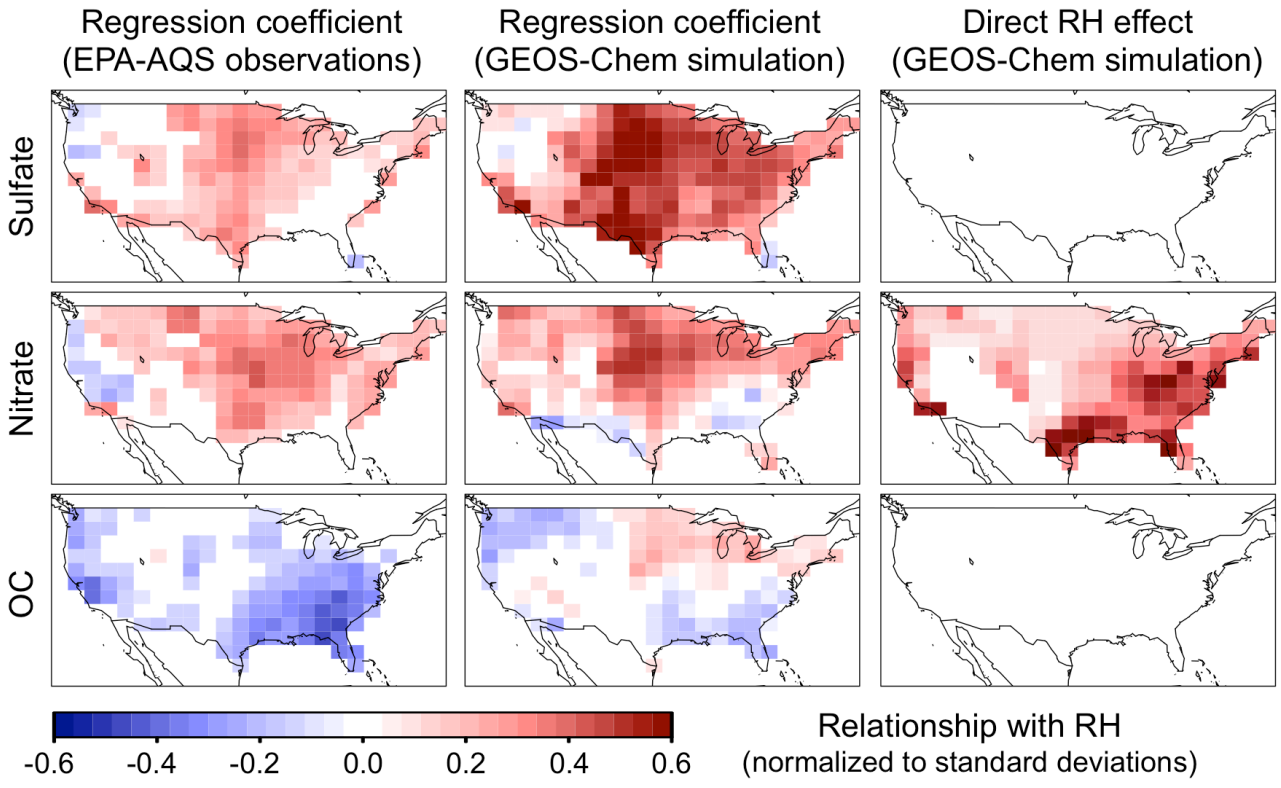

Fig. 4. Same as Fig. 3 but for relative humidity (RH). The right panels show the direct effects of RH as determined by applying a global −1 % RH perturbation in the GEOS-Chem simulation.

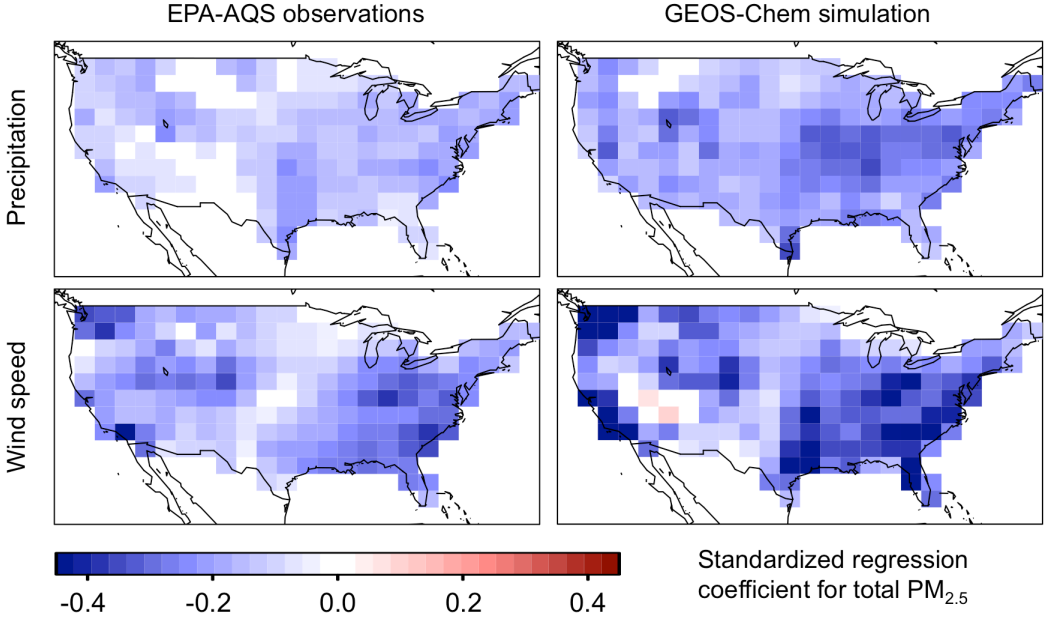

Fig. 5. Relationships of total $PM_{2.5}$ concentrations with precipitation and wind speed, expressed as the standardized regression coefficients β_3 and β_6, respectively. The left panels show observations (2004–2008) and the right panels model values (2005–2007). Values are for deseasonalized and detrended variables and are only shown when significant with 95 % confidence (p-value < 0.05).

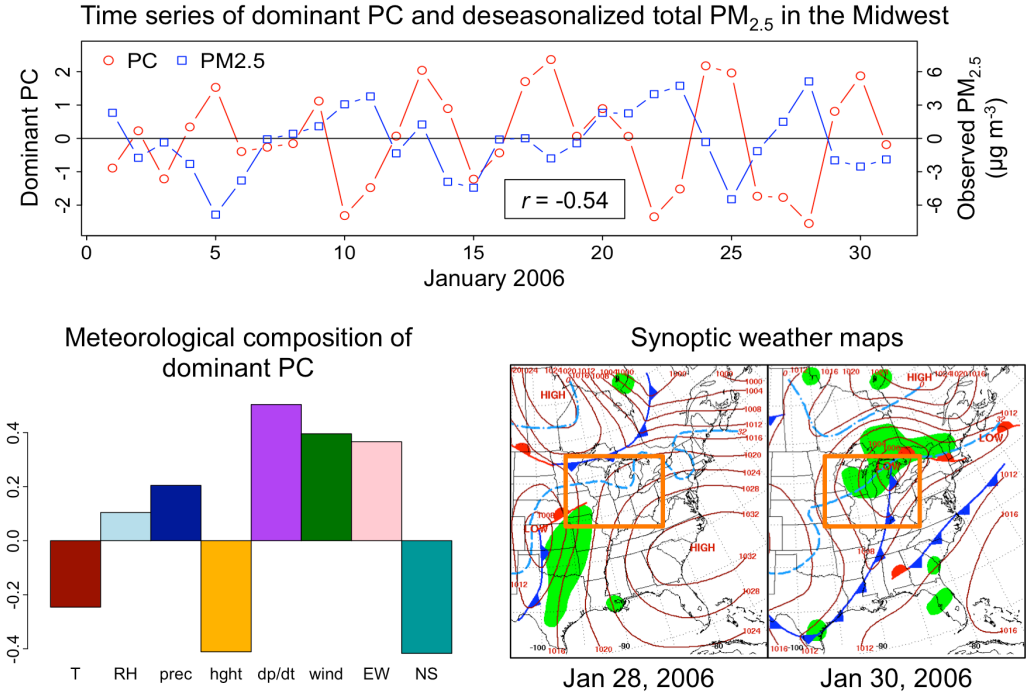

Fig. 6. Dominant meteorological mode for observed $PM_{2.5}$ variability in the Midwest inferred from the principal component analysis. Top panel: time series of deseasonalized observed total $PM_{2.5}$ concentrations and the dominant meteorological mode or principal component (PC) in January 2006. Bottom left: composition of this dominant mode as measured by the coefficients α_{ki} in Eq. (3). Meteorological variables (x_k) are listed in Table 1. Bottom right: synoptic weather maps from the National Center for Environmental Prediction (NCEP) (http://www.hpc.ncep.noaa.gov/dailywxmap/) for 28 and 30 January, corresponding to maximum negative and positive influences from the principal component. The Midwest is delineated in orange.

We then applied a principal component regression (PCR) model to correlate observed and simulated $PM_{2.5}$ concentrations with the eight PCs for each region

$$\frac{Y(t)-\bar{Y}}{s_Y} = \sum_{j=1}^{8} \gamma_j U_j(t) \tag{4}$$

where Y represents the regionally averaged $PM_{2.5}$ concentration, γ_j the PC regression coefficients, and $\bar{Y}$ and s_Y the temporal mean and standard deviation of Y. The ratio of regression to total sum of squares (SSR_j/SST) for each PC is calculated by

$$\frac{SSR_j}{SST} = \frac{\sum_t \left[\gamma_j U_j(t)\right]^2}{\sum_t \left\{\left[Y(t)-\bar{Y}\right]/s_Y\right\}^2} \tag{5}$$

where the summation is over the entire time series $Y(t)$ and $U_j(t)$. This ratio quantifies the fraction of variance of $PM_{2.5}$ that can be explained by a single PC. From Eqs. (3) and (4), the fraction (f_k) of the overall correlation of $PM_{2.5}$ with a given meteorological variable X_k (e.g., in Figs. 4 through 6) that is associated with a particular PC can be estimated by

$$f_k = \frac{\alpha_{kj}\gamma_j}{\sum_m \alpha_{km}\gamma_m} \tag{6}$$

where the summation is over the m PCs that have a significant effect on $PM_{2.5}$ (p-value < 0.01). Here the denominator represents the total effect of X_k on $PM_{2.5}$ that is equivalent to a regionally averaged version of β_k in Eq. (1). The PCR model was applied to both the full-year data and to seasonal subsets.

4.2 Dominant meteorological modes of $PM_{2.5}$ variability

Figure 6 shows as an example the dominant meteorological mode contributing to total $PM_{2.5}$ variability in the Midwest as determined by the highest SSR_j/SST ratio in Eq. (5). Based on the PCR model this mode alone explains 29 % of the observed $PM_{2.5}$ variability with a regression coefficient $\gamma_j = -0.41$. The top panel of Fig. 6 shows the time series of this mode for January 2006 together with the deseasonalized observed total $PM_{2.5}$ concentrations, illustrating strong

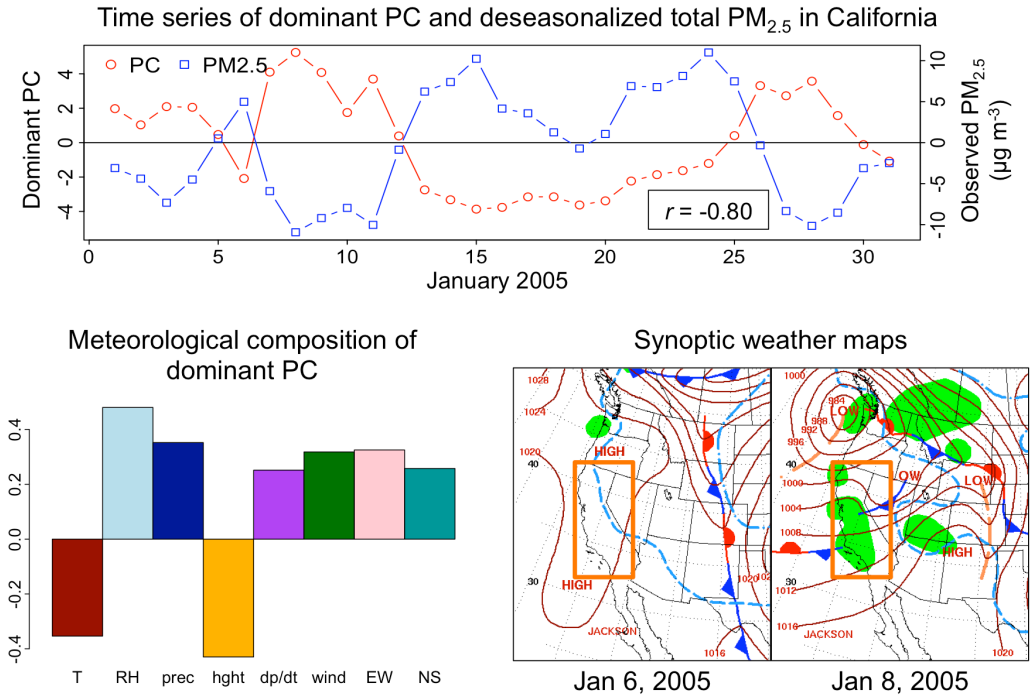

Fig. 7. Same as Fig. 6 but for California.

anticorrelation ($r = -0.54$). The bottom left panel shows the meteorological composition of this dominant mode as measured by PC coefficients α_{kj} in Eq. (3), consisting of low temperature, high precipitation, low and rising pressure, and strong northwesterly winds. From weather maps we can verify that high positive values of this PC represent the center of an eastward-propagating mid-latitude cyclone with a precipitating cold front at the southwest tail end. High negative values indicate the "opposite" regime – warm and dry stagnant condition at the tail end of an anticyclone. Figure 6 (top and bottom right) shows, for instance, that as $U_j(t)$ rose from a minimum to maximum between 28 and 30 January 2006 in the Midwest, a mid-latitude cyclone was approaching and the associated cold front swept over the region bringing down total $PM_{2.5}$ by 9 $\mu g\,m^{-3}$.

Figure 7 shows as another example the dominant meteorological mode of $PM_{2.5}$ variability in California, demonstrating again a strong anticorrelation between the time series of this mode and $PM_{2.5}$ concentrations ($r = -0.80$). This mode has similar meteorological composition to that in Fig. 6 except for wind direction. Positive phases of this mode represent ventilation by cold maritime inflows associated with synoptic disturbances, whereas negative phases represent warm, stagnant conditions associated with high-pressure systems. The bottom panel shows, for instance, that between 6 and 8 January 2005, a precipitating maritime inflow reduced $PM_{2.5}$ by 16 $\mu g\,m^{-3}$.

The analysis above was conducted for all regions of Fig. 1. Figures similar to Figs. 6 and 7 for other regions are included in the Supplement. Table 2 summarizes the characteristics of the dominant PC controlling $PM_{2.5}$ variability for five selected regions. In the eastern US (Northeast, Midwest and Southeast), the observed dominant modes resemble that for the Midwest described above (Fig. 6). In the Northeast, another mode representing southwesterlies associated with high pressure over the western North Atlantic is equally important. In the Pacific Northwest, the dominant mode resembles that for California (Fig. 7). In general, the PCR results illustrate the importance of synoptic-scale transport in controlling the observed daily variability of $PM_{2.5}$. As shown in Table 2, this control appears to be well represented in GEOS-Chem, supporting the ability of the model to describe the variability in $PM_{2.5}$ associated with this transport.

Using Eq. (6), we find overall that the synoptic transport modes account for more than 70 % of the observed correlations of $PM_{2.5}$ components with temperature in the Northeast and Midwest. This reflects the association of elevated temperature with southerly flow and stagnation. In the Southeast, however, we find that more than 60 % of the observed correlations of nitrate and OC with temperature and RH arise from a single non-transport mode consisting of low temperature and high RH. Nitrate has a positive dependence on that mode because of ammonium nitrate thermodynamics, while OC has a negative dependence reflecting biogenic VOC emissions and the occurrence of fires. The weaker importance

of transport in driving the nitrate-temperature relationship in the Southeast likely reflects the lower frequency of cold fronts. In California, the transport and non-transport modes are comparably important in shaping the observed correlations of $PM_{2.5}$ components with temperature and RH.

5 Cyclone frequency as a metric for climate change effect on $PM_{2.5}$

Mid-latitude cyclones and their associated cold fronts are known to provide the dominant year-round mechanism for ventilating the US Midwest and Northeast (Cooper et al., 2001; Li et al., 2005), and they emerge in our analysis of Sect. 4 as the dominant meteorological mode of $PM_{2.5}$ variability. Previous studies diagnosing cyclone frequency have relied on identifying local pressure minima (Mickley et al., 2004; Lambert and Fyfe, 2006; Lang and Waugh, 2011) or used storm tracking algorithms (Geng and Sugi, 2001; Bauer and Del Genio, 2006; Bengtsson et al., 2006). Here we diagnose cyclone frequency by applying a fast Fourier transform (FFT) to the time series of the dominant Midwest PC representing cyclone and frontal passages as shown in Fig. 6. We use 1999–2010 meteorological data from the NCEP/NCAR Reanalysis 1 (Kalnay et al., 1996; Kistler et al., 2001), which provides a longer record than GEOS-5. PCA of the NCEP/NCAR data yields essentially the same meteorological modes as GEOS-5. Figure 8 (gray thin line) shows the FFT spectrum for the dominant cyclone mode in the Midwest for 1999–2010. The low-frequency structure (with periods > 20 d) is an artifact of the 30-day moving average applied to the meteorological data to remove seasonality. We smooth the time series with a second-order autoregressive (AR2) filter (Wilks, 2006), indicating a median spectral frequency of $52\,a^{-1}$ (cyclone period of about 7 days).

We applied the spectral-autoregressive method above to find the median cyclone frequencies and periods for individual years of the 1999–2010 record. Figure 9 shows the time series of annual mean anomalies in total $PM_{2.5}$ concentrations and cyclone periods for the Midwest, where the correlation is strongest ($r = 0.76$) corresponding to a $PM_{2.5}$-to-cyclone period sensitivity of $0.94 \pm 0.43\,\mu g\,m^{-3}\,d^{-1}$ (95 % confidence interval). Leibensperger et al. (2008) previously found a strong interannual correlation of summer ozone with cyclone frequency in the Northeast using the 1980–2006 record of NCEP/NCAR data. Our analysis does not show the same for $PM_{2.5}$ in this region, possibly because of the short record (12 years) available for $PM_{2.5}$. Cyclone frequencies found by Leibensperger et al. (2008) are generally lower, possibly because their storm-tracking algorithm may neglect weaker cyclones and fronts.

The strong interannual correlation of $PM_{2.5}$ with cyclone frequency, at least in the Midwest, encourages the use of cyclone frequency as a metric to diagnose the effect of climate change on $PM_{2.5}$. We used for this purpose an ensemble of five realizations of 1950–2050 climate change generated by Leibensperger et al. (2011b) with the GISS GCM III (Rind et al., 2007) applied to the IPCC A1B scenario (Nakicenovic and Swart, 2000) and including time-dependent aerosol radiative forcings. For each realization we examined the change in median cyclone frequency between the present-day (1996–2010) and the future (2036–2050), by applying the spectral-autoregressive method to the dominant cyclone PC for each 15-year time series, and using a Monte Carlo method to diagnose the probability distribution and significance of the change based on variability of the AR2 parameters. Three out of the five realizations indicated statistically significant decreases in cyclone frequencies between 1996–2010 and 2036–2050 of -3.2, -3.4 and $-1.5\,a^{-1}$ (p-value < 0.05). One realization showed a significant increase of $2.7\,a^{-1}$ and another showed no significant change. Figure 10 shows the combined probability distribution of cyclone frequency change in the Midwest from all five realizations and the corresponding responses of annual mean $PM_{2.5}$ based on the $PM_{2.5}$-to-cyclone period sensitivity reported above, indicating a roughly 70 % probability of reduced cyclone frequency and elevated $PM_{2.5}$ in the Midwest by 2050. This corresponds to a mean decrease in cyclone frequency of $-1.1 \pm 4.8\,a^{-1}$ and a resulting increase in annual mean $PM_{2.5}$ of $0.13 \pm 0.60\,\mu g\,m^{-3}$.

Previous GISS-GEOS-Chem GCM-CTM studies of the effects of 2000–2050 climate change on $PM_{2.5}$ air quality projected a mean increase of 0.1–0.5 $\mu g\,m^{-3}$ in the Midwest in the 2050 climate based on one GCM realization (Pye et al., 2009; Lam et al., 2011). Their estimates are within the range of our projection from the cyclone frequency trend alone. However, the large variability of the cyclone trends (including in sign) across five realizations of the same GCM underscores the imperative need for multiple realizations in diagnosing the effect of climate change on $PM_{2.5}$ air quality. All GCM-CTM studies in the literature reviewed by Jacob and Winner (2009) have used single climate realizations and this may partly explain the inconsistency in their results.

Other climatic factors than cyclone and frontal frequency may also affect future $PM_{2.5}$ air quality in the US. Mean temperature increases may be particularly important for the Southeast as discussed previously. Changes in precipitation and PBL depth are obviously important. As scavenging within a precipitating column is highly efficient (Balkanski et al., 1993), precipitation frequency, often modulated by synoptic weather, may be more relevant as a predictor than climatological mean precipitation.

6 Conclusions

Projecting the effects of climate change on $PM_{2.5}$ air quality requires an understanding of the dependence of $PM_{2.5}$ on meteorological variables. We used here a multiple linear regression model to correlate both observed (EPA-AQS) and

Table 2. Dominant meteorological modes for regional $PM_{2.5}$ variability.

US Region	$PM_{2.5}$ variability explained [a]		PC regression coefficient γ_j [b]		Description [c]
	EPA-AQS	GEOS-Chem	EPA-AQS	GEOS-Chem	
Northeast	17 %	21 %	−0.31	−0.33	Cold front
Midwest	29 %	25 %	−0.41	−0.38	associated with
Southeast	31 %	15 %	−0.42	−0.29	mid-latitude cyclone
Pacific NW	36 %	45 %	−0.35	−0.39	Synoptic-scale
California	26 %	13 %	−0.28	−0.21	maritime inflow

[a] From Eq. (5).
[b] From Eq. (4).
[c] For positive phases of the dominant PC.

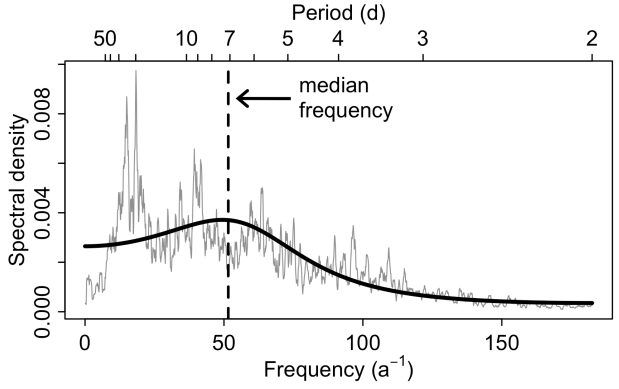

Fig. 8. Frequency spectrum of the daily time series of the dominant meteorological mode (cyclone/frontal passages) in the US Midwest (Fig. 1) for 1999–2010 using NCEP/NCAR Reanalysis 1 data. The thin line shows the fast Fourier transform (FFT) spectrum and the thick line shows the smoothed spectrum from a second-order autoregressive (AR2) model. The vertical dashed line indicates the median AR2 spectral frequency used as a metric of cyclone frequency.

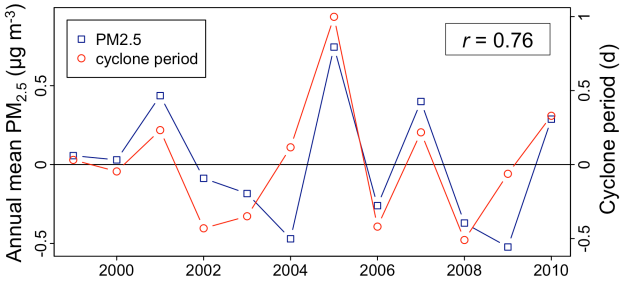

Fig. 9. Anomalies of annual mean $PM_{2.5}$ concentrations and median cyclone periods for the US Midwest (Fig. 1).

simulated (GEOS-Chem) daily mean concentrations of total $PM_{2.5}$ and its major components with a suite of meteorological variables in the contiguous US for 2004–2008. All data were deseasonalized to focus on synoptic correlations. We applied principal component analysis (PCA) and regression to identify the dominant meteorological modes controlling $PM_{2.5}$ variability, and showed how trend analysis for these modes can be used to estimate the effects of climate change on $PM_{2.5}$.

We observe strong positive correlations of all $PM_{2.5}$ components with temperature in most of the US, except for nitrate in the Southeast where the correlation is negative. A temperature perturbation simulation with GEOS-Chem reveals that most of the correlations of $PM_{2.5}$ with temperature do not arise from direct dependence on temperature but from covariation with synoptic transport. Exceptions are nitrate and OC in the Southeast, where the direct dependence of ammonium nitrate thermodynamics and biogenic VOC emissions on temperature contributes significantly to the correlations. RH is generally positively correlated with sulfate and nitrate but negatively correlated with OC; the correlations also appear to be mainly driven by covariation of RH with synoptic transport. Total $PM_{2.5}$ is strongly negatively correlated everywhere with precipitation and wind speed.

We find from the PCA and regression that 20–40 % of the observed $PM_{2.5}$ day-to-day variability in different US regions can be explained by a single dominant synoptic meteorological mode: cold frontal passages in the eastern US and maritime inflow in the West. These and other transport modes are found to contribute to most of the overall correlations of different $PM_{2.5}$ components with temperature and RH except in the Southeast.

We show that the interannual variability of annual mean $PM_{2.5}$ in the Midwest for 1999–2010 is strongly correlated with cyclone frequency as diagnosed from a spectral-autoregressive analysis of the dominant meteorological mode of variability, with a $PM_{2.5}$-to-cyclone period sensitivity of $0.9 \pm 0.4\,\mu g\,m^{-3}\,d^{-1}$. We conducted an ensemble of five realizations of 1996–2050 climate change using the GISS GCM III with A1B greenhouse and aerosol forcings. Three of these found a significant decrease in cyclone frequency

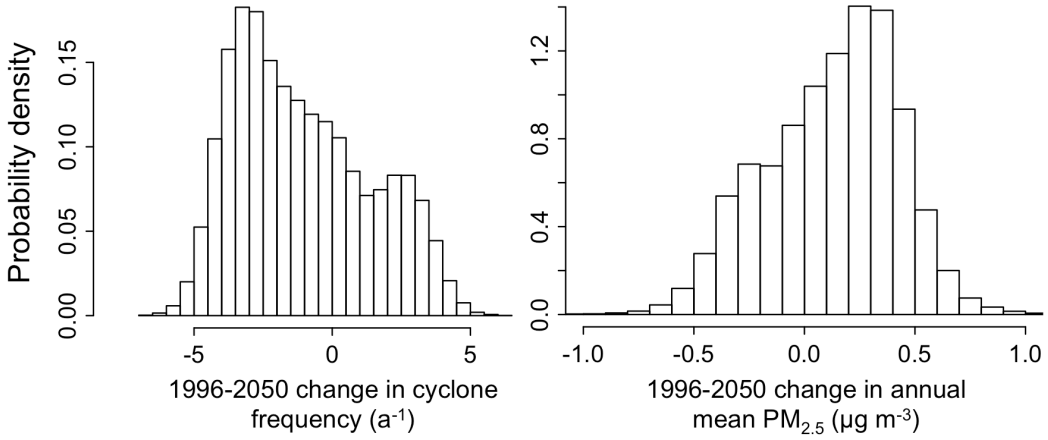

Fig. 10. Probability distribution for the change in median cyclone frequency in the US Midwest between 1996–2010 and 2036–2050, and the corresponding change in annual mean $PM_{2.5}$ concentrations. Results are from five realizations of the NASA Goddard Institute for Space Studies (GISS) GCM III applied to the IPCC A1B scenario of greenhouse gas and aerosol forcings.

over the US Midwest, one found no significant change and one found a significant increase. From this ensemble we derive a likely increase in annual mean $PM_{2.5}$ of $0.13 \pm 0.60\,\mu g\,m^{-3}$ in the Midwest in the 2050s climate. This is consistent with previous GCM-CTM studies using the same GCM and suggests that cyclone frequency may be a major driver of the effect of climate change on $PM_{2.5}$ air quality. However, the variability of cyclone trends (including in sign) across multiple realizations of the same GCM with identical forcings demonstrates the importance of multiple climate change realizations in GCM-CTM studies because of climate chaos. All GCM-CTM studies to date have used single realizations because of computational expense, and this may partly explain the wide inconsistencies in their projections of $PM_{2.5}$ response to climate change. The climate trend analysis in this study, using the Midwest as an illustration, is preliminary. A comprehensive analysis using outputs from various GCMs will be the topic of a future paper.

Supplementary material related to this article is available online at: http://www.atmos-chem-phys.net/12/3131/2012/acp-12-3131-2012-supplement.pdf.

Acknowledgements. This work was supported by a Mustard Seed Foundation Harvey Fellowship to Amos P. K. Tai, and the NASA Applied Sciences Program through the NASA Air Quality Applied Sciences Team (AQAST). Although this paper has been reviewed by the EPA and approved for publication, it does not necessarily reflect EPA's policies or views.

Edited by: D. J. Cziczo

References

Aw, J. and Kleeman, M. J.: Evaluating the first-order effect of intraannual temperature variability on urban air pollution, J. Geophys. Res.-Atmos., 108, 4365, doi:10.1029/2002jd002688, 2003.

Balkanski, Y. J., Jacob, D. J., Gardner, G. M., Graustein, W. C., and Turekian, K. K.: Transport and residence times of tropospheric aerosols inferred from a global 3-dimensional simulation of pb-210, J. Geophys. Res.-Atmos., 98, 20573–20586, 1993.

Bauer, M. and Del Genio, A. D.: Composite analysis of winter cyclones in a gcm: Influence on climatological humidity, J. Climate, 19, 1652–1672, 2006.

Bengtsson, L., Hodges, K. I., and Roeckner, E.: Storm tracks and climate change, J. Climate, 19, 3518–3543, 2006.

Bertram, T. H., Heckel, A., Richter, A., Burrows, J. P., and Cohen, R. C.: Satellite measurements of daily variations in soil nox emissions, Geophys. Res. Lett., 32, L24812, doi:10.1029/2005gl024640, 2005.

Chen, D., Wang, Y., McElroy, M. B., He, K., Yantosca, R. M., and Le Sager, P.: Regional CO pollution and export in China simulated by the high-resolution nested-grid GEOS-Chem model, Atmos. Chem. Phys., 9, 3825–3839, doi:10.5194/acp-9-3825-2009, 2009.

Cheng, C. S. Q., Campbell, M., Li, Q., Li, G. L., Auld, H., Day, N., Pengelly, D., Gingrich, S., and Yap, D.: A synoptic climatological approach to assess climatic impact on air quality in south-central canada. Part ii: Future estimates, Water Air Soil Poll., 182, 117–130, 2007.

Christensen, J. H., Hewitson, B., Busuioc, A., Chen, A., Gao, X., Held, I., Jones, R., Kolli, R. K., Kwon, W.-T., Laprise, R., Magana Rueda, V., Mearns, L., Menendez, C. G., Raisanen, J., Rinke, A., Sarr, A., and Whetton, P.: Regional climate projections, in: Climate change 2007: The physical science basis. Contribution of working group i to the fourth assessment report of the intergovernmental panel on climate change, Cambridge University Press, New York, NY, USA, 847–940, 2007.

Chung, S. H. and Seinfeld, J. H.: Global distribution and climate

forcing of carbonaceous aerosols, J. Geophys. Res.-Atmos., 107, 4407, doi:10.1029/2001jd001397, 2002.

Cooke, W. F., Liousse, C., Cachier, H., and Feichter, J.: Construction of a 1 degrees × 1 degrees fossil fuel emission data set for carbonaceous aerosol and implementation and radiative impact in the echam4 model, J. Geophys. Res.-Atmos., 104, 22137–22162, 1999.

Cooper, O. R., Moody, J. L., Parrish, D. D., Trainer, M., Ryerson, T. B., Holloway, J. S., Hubler, G., Fehsenfeld, F. C., Oltmans, S. J., and Evans, M. J.: Trace gas signatures of the airstreams within north atlantic cyclones: Case studies from the north atlantic regional experiment (nare '97) aircraft intensive, J. Geophys. Res.-Atmos., 106, 5437–5456, 2001.

Dawson, J. P., Adams, P. J., and Pandis, S. N.: Sensitivity of $PM_{2.5}$ to climate in the Eastern US: a modeling case study, Atmos. Chem. Phys., 7, 4295–4309, doi:10.5194/acp-7-4295-2007, 2007.

Day, M. C. and Pandis, S. N.: Predicted changes in summertime organic aerosol concentrations due to increased temperatures, Atmos. Environ., 45, 6546–6556, 2011.

Drury, E., Jacob, D. J., Spurr, R. J. D., Wang, J., Shinozuka, Y., Anderson, B. E., Clarke, A. D., Dibb, J., McNaughton, C., and Weber, R.: Synthesis of satellite (modis), aircraft (icartt), and surface (improve, epa-aqs, aeronet) aerosol observations over eastern north america to improve modis aerosol retrievals and constrain surface aerosol concentrations and sources, J. Geophys. Res.-Atmos., 115, D14204, doi:10.1029/2009JD012629, 2010.

Fang, Y., Fiore, A. M., and Horowitz, L. W.: Impacts of changing transport and precipitation on pollutant distribution in a future climate, J. Geophys. Res.-Atmos., 116, D18303, doi:10.1029/2011JD015642, 2011.

Fisher, J. A., Jacob, D. J., Wang, Q., Bahreini, R., Carouge, C. C., Cubison, M. J., Dibb, J. E., Diehl, T., Jimenez, J. L., Leibensperger, E. M., Meinders, M. B. J., Pye, H. O. T., Quinn, P. K., Sharma, S., van Donkelaar, A., and Yantosca, R. M.: Sources, distribution, and acidity of sulfate-ammonium aerosol in the arctic in winter-spring, Atmos. Environ., 45, 7301–7318, 2011.

Fountoukis, C. and Nenes, A.: ISORROPIA II: a computationally efficient thermodynamic equilibrium model for $K^+Ca^{2+}Mg^{2+}NH_4^+Na^+SO_4^{2-}NO_3^-Cl^-H_2O$ aerosols, Atmos. Chem. Phys., 7, 4639–4659, doi:10.5194/acp-7-4639-2007, 2007.

Fu, T. M., Jacob, D. J., and Heald, C. L.: Aqueous-phase reactive uptake of dicarbonyls as a source of organic aerosol over eastern north america, Atmos. Environ., 43, 1814–1822, 2009.

Geng, Q. Z. and Sugi, M.: Variability of the north atlantic cyclone activity in winter analyzed from ncep-ncar reanalysis data, J. Climate, 14, 3863–3873, 2001.

Giglio, L., van der Werf, G. R., Randerson, J. T., Collatz, G. J., and Kasibhatla, P.: Global estimation of burned area using MODIS active fire observations, Atmos. Chem. Phys., 6, 957–974, doi:10.5194/acp-6-957-2006, 2006.

Guenther, A., Karl, T., Harley, P., Wiedinmyer, C., Palmer, P. I., and Geron, C.: Estimates of global terrestrial isoprene emissions using MEGAN (Model of Emissions of Gases and Aerosols from Nature), Atmos. Chem. Phys., 6, 3181–3210, doi:10.5194/acp-6-3181-2006, 2006.

Heald, C. L., Jacob, D. J., Park, R. J., Alexander, B., Fairlie, T. D., Yantosca, R. M., and Chu, D. A.: Transpacific transport of asian anthropogenic aerosols and its impact on surface air quality in the united states, J. Geophys. Res.-Atmos., 111, D14310, doi:10.1029/2005JD006847, 2006.

Heald, C. L., Henze, D. K., Horowitz, L. W., Feddema, J., Lamarque, J. F., Guenther, A., Hess, P. G., Vitt, F., Seinfeld, J. H., Goldstein, A. H., and Fung, I.: Predicted change in global secondary organic aerosol concentrations in response to future climate, emissions, and land use change, J. Geophys. Res.-Atmos., 113, D05211, doi:10.1029/2007jd009092, 2008.

Henze, D. K., Seinfeld, J. H., Ng, N. L., Kroll, J. H., Fu, T.-M., Jacob, D. J., and Heald, C. L.: Global modeling of secondary organic aerosol formation from aromatic hydrocarbons: high- vs. low-yield pathways, Atmos. Chem. Phys., 8, 2405–2420, doi:10.5194/acp-8-2405-2008, 2008.

Holtslag, A. A. M. and Boville, B. A.: Local versus nonlocal boundary-layer diffusion in a global climate model, J. Climate, 6, 1825–1842, 1993.

Jacob, D. J. and Winner, D. A.: Effect of climate change on air quality, Atmos. Environ., 43, 51–63, 2009.

Jacob, D. J., Logan, J. A., Gardner, G. M., Yevich, R. M., Spivakovsky, C. M., Wofsy, S. C., Sillman, S., and Prather, M. J.: Factors regulating ozone over the united-states and its export to the global atmosphere, J. Geophys. Res.-Atmos., 98, 14817–14826, 1993.

Kalnay, E., Kanamitsu, M., Kistler, R., Collins, W., Deaven, D., Gandin, L., Iredell, M., Saha, S., White, G., Woollen, J., Zhu, Y., Chelliah, M., Ebisuzaki, W., Higgins, W., Janowiak, J., Mo, K. C., Ropelewski, C., Wang, J., Leetmaa, A., Reynolds, R., Jenne, R., and Joseph, D.: The ncep/ncar 40-year reanalysis project, B. Am. Meteorol. Soc., 77, 437–471, 1996.

Kistler, R., Kalnay, E., Collins, W., Saha, S., White, G., Woollen, J., Chelliah, M., Ebisuzaki, W., Kanamitsu, M., Kousky, V., van den Dool, H., Jenne, R., and Fiorino, M.: The ncep-ncar 50-year reanalysis: Monthly means cd-rom and documentation, B. Am. Meteorol. Soc., 82, 247–267, 2001.

Kleeman, M. J.: A preliminary assessment of the sensitivity of air quality in california to global change, Climatic Change, 87, S273–S292, doi:10.1007/S10584-007-9351-3, 2008.

Koch, D., Park, J., and Del Genio, A.: Clouds and sulfate are anticorrelated: A new diagnostic for global sulfur models, J. Geophys. Res.-Atmos., 108, 4781, doi:10.1029/2003jd003621, 2003.

Kutner, M. H., Nachtsheim, C., and Neter, J.: Applied linear regression models, 4th Edn., McGraw-Hill/Irwin, Boston, New York, USA, 701 pp., 2004.

Lam, Y. F., Fu, J. S., Wu, S., and Mickley, L. J.: Impacts of future climate change and effects of biogenic emissions on surface ozone and particulate matter concentrations in the United States, Atmos. Chem. Phys., 11, 4789–4806, doi:10.5194/acp-11-4789-2011, 2011.

Lambert, S. J. and Fyfe, J. C.: Changes in winter cyclone frequencies and strengths simulated in enhanced greenhouse warming experiments: Results from the models participating in the ipcc diagnostic exercise, Clim. Dynam., 26, 713–728, 2006.

Lang, C. and Waugh, D. W.: Impact of climate change on the frequency of northern hemisphere summer cyclones, J. Geophys. Res.-Atmos., 116, D04103, doi:10.1029/2010JD014300, 2011.

Leibensperger, E. M., Mickley, L. J., and Jacob, D. J.: Sensitivity of US air quality to mid-latitude cyclone frequency and implications of 1980–2006 climate change, Atmos. Chem. Phys., 8,

7075–7086, doi:10.5194/acp-8-7075-2008, 2008.

Leibensperger, E. M., Mickley, L. J., Jacob, D. J., Chen, W.-T., Seinfeld, J. H., Nenes, A., Adams, P. J., Streets, D. G., Kumar, N., and Rind, D.: Climate effects of 1950–2050 changes in us anthropogenic aerosols – part 1: Aerosol trends and radiative forcing, Atmos. Chem. Phys., accepted, 2011a.

Leibensperger, E. M., Mickley, L. J., Jacob, D. J., Chen, W.-T., Seinfeld, J. H., Nenes, A., Adams, P. J., Streets, D. G., Kumar, N., and Rind, D.: Climate effects of 1950–2050 changes in us anthropogenic aerosols – part 2: Climate response, Atmos. Chem. Phys., in press, 2011b.

Li, Q. B., Jacob, D. J., Park, R., Wang, Y. X., Heald, C. L., Hudman, R., Yantosca, R. M., Martin, R. V., and Evans, M.: North american pollution outflow and the trapping of convectively lifted pollution by upper-level anticyclone, J. Geophys. Res.-Atmos., 110, D10301, doi:10.1029/2004jd005039, 2005.

Liao, H., Chen, W. T., and Seinfeld, J. H.: Role of climate change in global predictions of future tropospheric ozone and aerosols, J. Geophys. Res.-Atmos., 111, D12304, doi:10.1029/2005jd006852, 2006.

Liao, H., Henze, D. K., Seinfeld, J. H., Wu, S. L., and Mickley, L. J.: Biogenic secondary organic aerosol over the united states: Comparison of climatological simulations with observations, J. Geophys. Res.-Atmos., 112, D06201, doi:10.1029/2006jd007813, 2007.

Lin, J. T. and McElroy, M. B.: Impacts of boundary layer mixing on pollutant vertical profiles in the lower troposphere: Implications to satellite remote sensing, Atmos. Environ., 44, 1726–1739, 2010.

Liu, H. Y., Jacob, D. J., Bey, I., and Yantosca, R. M.: Constraints from pb-210 and be-7 on wet deposition and transport in a global three-dimensional chemical tracer model driven by assimilated meteorological fields, J. Geophys. Res.-Atmos., 106, 12109–12128, 2001.

Mickley, L. J., Jacob, D. J., Field, B. D., and Rind, D.: Effects of future climate change on regional air pollution episodes in the united states, Geophys. Res. Lett., 31, L24103, doi:10.1029/2004gl021216, 2004.

Murazaki, K. and Hess, P.: How does climate change contribute to surface ozone change over the united states?, J. Geophys. Res.-Atmos., 111, D05301, doi:10.1029/2005jd005873, 2006.

Nakicenovic, N. and Swart, R.: Special report on emissions scenarios: A special report of working group iii of the intergovernmental panel on climate change, Cambridge University Press, Cambridge, New York, USA, 599 pp., 2000.

Park, R. J., Jacob, D. J., Field, B. D., Yantosca, R. M., and Chin, M.: Natural and transboundary pollution influences on sulfate-nitrate-ammonium aerosols in the united states: Implications for policy, J. Geophys. Res.-Atmos., 109, D15204, doi:10.1029/2003jd004473, 2004.

Park, R. J., Jacob, D. J., Kumar, N., and Yantosca, R. M.: Regional visibility statistics in the united states: Natural and transboundary pollution influences, and implications for the regional haze rule, Atmos. Environ., 40, 5405–5423, 2006.

Park, R. J., Jacob, D. J., and Logan, J. A.: Fire and biofuel contributions to annual mean aerosol mass concentrations in the united states, Atmos. Environ., 41, 7389–7400, 2007.

Pinder, R. W., Pekney, N. J., Davidson, C. I., and Adams, P. J.: A process-based model of ammonia emissions from dairy cows: Improved temporal and spatial resolution, Atmos. Environ., 38, 1357–1365, 2004.

Pinto, J. G., Ulbrich, U., Leckebusch, G. C., Spangehl, T., Reyers, M., and Zacharias, S.: Changes in storm track and cyclone activity in three sres ensemble experiments with the echam5/mpi-om1 gcm, Clim. Dynam., 29, 195–210, 2007.

Pye, H. O. T., Liao, H., Wu, S., Mickley, L. J., Jacob, D. J., Henze, D. K., and Seinfeld, J. H.: Effect of changes in climate and emissions on future sulfate-nitrate-ammonium aerosol levels in the united states, J. Geophys. Res.-Atmos., 114, D01205, doi:10.1029/2008jd010701, 2009.

Rasmussen, D. J., Fiore, A. M., Naik, V., Horowitz, L. W., McGinnis, S. J., and Schultz, M. G.: Surface ozone-temperature relationships in the eastern us: A monthly climatology for evaluating chemistry-climate models, Atmos. Environ., 47, 142–153, doi:10.1016/j.atmosenv.2011.11.021, 2012.

Rind, D., Lerner, J., Jonas, J., and McLinden, C.: Effects of resolution and model physics on tracer transports in the nasa goddard institute for space studies general circulation models, J. Geophys. Res.-Atmos., 112, D09315, doi:10.1029/2006jd007476, 2007.

Sheehan, P. E. and Bowman, F. M.: Estimated effects of temperature on secondary organic aerosol concentrations, Environ. Sci. Technol., 35, 2129–2135, 2001.

Sillman, S. and Samson, F. J.: Impact of temperature on oxidant photochemistry in urban, polluted rural and remote environments, J. Geophys. Res.-Atmos., 100, 11497–11508, 1995.

Spracklen, D. V., Mickley, L. J., Logan, J. A., Hudman, R. C., Yevich, R., Flannigan, M. D., and Westerling, A. L.: Impacts of climate change from 2000 to 2050 on wildfire activity and carbonaceous aerosol concentrations in the western united states, J. Geophys. Res.-Atmos., 114, D20301, doi:10.1029/2008jd010966, 2009.

Stelson, A. W. and Seinfeld, J. H.: Relative-humidity and temperature-dependence of the ammonium-nitrate dissociation-constant, Atmos. Environ., 16, 983–992, 1982.

Tai, A. P. K., Mickley, L. J., and Jacob, D. J.: Correlations between fine particulate matter ($pm_{2.5}$) and meteorological variables in the united states: Implications for the sensitivity of $pm_{2.5}$ to climate change, Atmos. Environ., 44, 3976–3984, 2010.

Thishan Dharshana, K. G., Kravtsov, S., and Kahl, J. D. W.: Relationship between synoptic weather disturbances and particulate matter air pollution over the united states, J. Geophys. Res.-Atmos., 115, D24219, doi:10.1029/2010jd014852, 2010.

van Donkelaar, A., Martin, R. V., and Park, R. J.: Estimating ground-level pm(2.5) using aerosol optical depth determined from satellite remote sensing, J. Geophys. Res.-Atmos., 111, D21201, doi:10.1029/2005JD006996, 2006.

van Donkelaar, A., Martin, R. V., Leaitch, W. R., Macdonald, A. M., Walker, T. W., Streets, D. G., Zhang, Q., Dunlea, E. J., Jimenez, J. L., Dibb, J. E., Huey, L. G., Weber, R., and Andreae, M. O.: Analysis of aircraft and satellite measurements from the Intercontinental Chemical Transport Experiment (INTEX-B) to quantify long-range transport of East Asian sulfur to Canada, Atmos. Chem. Phys., 8, 2999–3014, doi:10.5194/acp-8-2999-2008, 2008.

Wang, Y. H., Jacob, D. J., and Logan, J. A.: Global simulation of tropospheric o-3-nox-hydrocarbon chemistry 1. Model formulation, J. Geophys. Res.-Atmos., 103, 10713–10725, 1998.

Weaver, C. P., Liang, X. Z., Zhu, J., Adams, P. J., Amar, P., Avise,

J., Caughey, M., Chen, J., Cohen, R. C., Cooter, E., Dawson, J. P., Gilliam, R., Gilliland, A., Goldstein, A. H., Grambsch, A., Grano, D., Guenther, A., Gustafson, W. I., Harley, R. A., He, S., Hemming, B., Hogrefe, C., Huang, H. C., Hunt, S. W., Jacob, D. J., Kinney, P. L., Kunkel, K., Lamarque, J. F., Lamb, B., Larkin, N. K., Leung, L. R., Liao, K. J., Lin, J. T., Lynn, B. H., Manomaiphiboon, K., Mass, C., McKenzie, D., Mickley, L. J., O'Neill, S. M., Nolte, C., Pandis, S. N., Racherla, P. N., Rosenzweig, C., Russell, A. G., Salathe, E., Steiner, A. L., Tagaris, E., Tao, Z., Tonse, S., Wiedinmyer, C., Williams, A., Winner, D. A., Woo, J. H., Wu, S., and Wuebbles, D. J.: A preliminary synthesis of modeled climate change impacts on us regional ozone concentrations, B. Am. Meteorol. Soc., 90, 1843–1863, 2009.

Wesely, M. L.: Parameterization of surface resistances to gaseous dry deposition in regional-scale numerical-models, Atmos. Environ., 23, 1293–1304, 1989.

Wilks, D. S.: Statistical methods in the atmospheric sciences, 2nd edn., International geophysics series, 91, Academic Press, Amsterdam, Boston, xvii, 627 pp., 2006.

Wise, E. K. and Comrie, A. C.: Meteorologically adjusted urban air quality trends in the southwestern united states, Atmos. Environ., 39, 2969–2980, 2005.

Wu, S., Mickley, L. J., Leibensperger, E. M., Jacob, D. J., Rind, D., and Streets, D. G.: Effects of 2000–2050 global change on ozone air quality in the united states, J. Geophys. Res.-Atmos., 113, D06302, doi:10.1029/2007jd008917, 2008.

Yienger, J. J. and Levy, H.: Empirical-model of global soil-biogenic NO_x emissions, J. Geophys. Res.-Atmos., 100, 11447–11464, 1995.

Zhang, L., Jacob, D. J., Downey, N. V., Wood, D. A., Blewitt, D., Carouge, C. C., van Donkelaar, A., Jones, D. B. A., Murray, L. T., and Wang, Y. X.: Improved estimate of the policy-relevant background ozone in the united states using the geos-chem global model with 1/2 degrees x 2/3 degrees horizontal resolution over north america, Atmos. Environ., 45, 6769–6776, doi:10.1016/J.Atmosenv.2011.07.054, 2011.

Zhang, L., Jacob, D. J., Knipping, E. M., Kumar, N., Munger, J. W., Carouge, C. C., van Donkelaar, A., Wang, Y. X., and Chen, D.: Nitrogen deposition to the United States: distribution, sources, and processes, Atmos. Chem. Phys. Discuss., 12, 241–282, doi:10.5194/acpd-12-241-2012, 2012.